Eur. Phys. J. B **8**, 377–387 (1999)

THE EUROPEAN PHYSICAL JOURNAL B

EDP Sciences
© Società Italiana di Fisica
Springer-Verlag 1999

Thermal evolution of hole dynamics in the large-dimensional t−J model

M.P.H. Stumpf and D.E. Logan[a]

University of Oxford, Physical and Theoretical Chemistry Laboratory, South Parks Road, Oxford OX1 3QZ, UK

Received 16 September 1998

Abstract. The dynamics of a single hole in the $t-J$ model is solved exactly for all temperature, T, in the limit of large spatial dimensions, $d = \infty$, using the Feenberg renormalized perturbation series. We focus in particular on single-particle spectra, together with optical and static hole conductivities. Explicit results are illustrated for a Bethe lattice, and exemplify the continuous thermal evolution of the underlying string picture from the $T = 0$ string-pinned limit through to the paramagnetic phase. Quenched site-disorder is also readily incorporated, exact results thereby being obtained for the interplay between disorder and thermally-induced hole dynamics.

PACS. 71.10.Fd Lattice fermion models (Hubbard model, etc.)

1 Introduction

The dynamics of a hole in an antiferromagnetic insulator, as described by the $t-J$ model [1], represents a classic example of a strongly correlated electron problem: hole motion, *via* a nearest neighbour hopping amplitude t, occurs in a restricted subspace of no doubly occupied sites and is strongly coupled to spin excitations of the underlying undoped insulator, themselves described by an antiferromagnetic Heisenberg model, $\hat{H}_J$, with nearest neighbour exchange coupling J. Stimulated in part by a desire to understand high-T_c superconducting materials at low hole doping, intense study of the $t-J$ model has ensued (reviewed *e.g.* in [2]), building upon early pioneering foundations [3–5].

The so-called string picture [5–10] has proven central to an understanding of the $t-J$ model at $T = 0$, and exemplifies the strong coupling between hole motion and the spin background. It arises clearly at the 'Ising level' wherein transverse (spin-flip) interactions in $\hat{H}_J$ are neglected. Here, since the Néel spin configuration is the $T = 0$ ground state for bipartite lattices, single-step hole motion (Fig. 1) incurs of necessity an exchange energy penalty at each step, generating a linear confining potential: subject to the neglect of Trugman loop paths [11], the hole is then localized by the string of upturned spins created by its motion in the Néel state. Spin-flip interactions in $\hat{H}_J$, as well as Trugman processes, induce string unwinding and hence a finite hole mobility, thus mitigating against the simple string picture. Nonetheless, as known in particular from numerical studies [2,12,13], the underlying string picture is robust even in low spatial dimensions, $d = 2$.

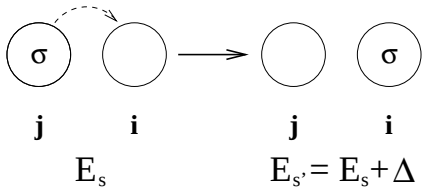

Fig. 1. Single-step hole motion as discussed in the text, with $E_s/E_{s'}$ the exchange energies of the spin background before/after the spin hop.

There is however another rather obvious mechanism, considered in this paper, that induces a finite hole mobility even in the Ising limit: temperature, T. This is clear since, for $T \gg J$ on which scale spin correlations are negligible, the $t-J$ model is in practice described by its $J = 0$ limit first studied many years ago [3,4], for which the string picture is irrelevant and wherein the hole propagates essentially as a free particle. Since the underlying spin background changes radically on a scale of $T \sim J$, hole dynamics thus evolve accordingly. The goal then is to describe the continuous thermal evolution of hole motion, recognizing that while two-sublattice AFLRO persists up to the Néel temperature T_N, all sites have a non-vanishing probability, for *any* finite temperature, of being occupied by a spin of either type ($\sigma = \uparrow$ or $\downarrow$). In consequence, and in contrast to $T = 0$ where hole-motion in the Néel configuration necessarily induces an exchange energy barrier, single-step hole motion at finite-T (Fig. 1) may incur either an exchange energy penalty *or* a gain, the latter processes leading naturally to a finite hole mobility.

[a] e-mail: dlogan@physchem.ox.ac.uk

We consider the $t-J$ model in the limit of large spatial dimensions, $d = \infty$, where rich results have already been obtained (see *e.g.* [14–18]), and study of which both admits the possibility of exact solutions and serves as a mean-field starting point for a systematic approach to the finite-d case. In particular, the large-dimensional limit has been solved at $T = 0$ [14,15] and the string picture shown to be exact. The primary physical reason for this is the total suppression of spatial fluctuations for $d = \infty$, whence spin excitations are purely Ising-like [15]; a characteristic which permits in consequence a 'clean' investigation of thermally induced hole mobility, in isolation from the analogous effects of the spin-flip interactions additionally operative in finite-d.

In this paper, a complement to a recent Letter [19], we show that an exact and physically transparent solution to the d^∞ $t-J$ model can be obtained for all temperatures. In Section 2, following a brief discussion of the thermal evolution of the pure spin background, we first consider (Sect. 2.1) the hole Green function and hence single-particle spectrum ($D(\omega)$) at finite temperature, and its connection to the usual time-ordered Green function for the half-filled state (one electron/site). The solution for the hole Green function is developed in Section 2.2, and given explicitly for the case of a Bethe lattice (whose topology underlies the well known retraceable path approximation [4] in finite-d). Here we employ the Feenberg renormalized perturbation series [20] that is familiar in relation to tight-binding models (see *e.g.* [21]), and whose use in the present context amounts to a renormalization of the Nagaoka path formalism [3,4]. The dynamical hole conductivity is considered in Section 2.3, exact results for which can be obtained in d^∞ due to the strict suppression of vertex corrections.

A subsidiary aim of the present work is also to study the influence of quenched site disorder and its interplay with thermally induced hole dynamics, an issue of importance in many magnetically disordered materials. The large-dimensional disordered $t-J$ model has hitherto been investigated by Strack and Vollhardt [15], in an approach that is exact at $T = 0$ alone. In Section 2.4 we show that an exact solution to this problem, for all T, follows from straightforward extension of the basic theory developed in Sections 2.2, 2.3. Detailed results for the single-particle spectra and hole conductivities (dynamic and static) are given respectively in Sections 3 and 4, for both the pure and disordered cases; and the paper concludes with a brief summary and outlook, Section 5.

2 Theory

The $t-J$ Hamiltonian, $\hat{H} = \hat{H}_t + \hat{H}_J$, is given by

$$\hat{H} = \sum_{i,j,\sigma} t_{ij} \tilde{c}^\dagger_{i\sigma} \tilde{c}_{j\sigma} + \frac{1}{2} J \sum_{i,j} \hat{\mathbf{S}}_i \cdot \hat{\mathbf{S}}_j, \tag{2.1}$$

where $\tilde{c}^\dagger_{i\sigma} = c^\dagger_{i\sigma}(1-\hat{n}_{i-\sigma})$ reflects the constraint to no double occupancy of sites by electrons; $J > 0$ is the nearest neighbour (NN) exchange coupling, with the corresponding lattice sum over NN sites on a bipartite lattice. In the pure $t-J$ model considered here the hopping matrix element t_{ij} likewise connects NN sites only: $t_{ij} = t$ for sites i and j NN's, and zero otherwise; and t and J are scaled as

$$t = t_*/\sqrt{Z}, \quad J = J_*/Z \tag{2.2}$$

with Z the coordination number ($= 2d$ for a hypercubic lattice), in order that the limit $d \to \infty$ be well defined. Transverse (spin-flip) interaction terms in $\hat{H}_J$ contribute only to $O(1/d)$ and are thus suppressed entirely for d^∞ [14,15]; *i.e.* only Ising-like spin interactions survive, whence in practice

$$\hat{H}_J \equiv \frac{1}{2} J \sum_{i,j} \hat{S}_{iz} \hat{S}_{jz}. \tag{2.3}$$

We first consider briefly the pure Heisenberg model, $\hat{H}_J$, since it is this that dictates the spin background in which the hole moves. The key feature of d^∞ is that simple molecular field theory is exact for the Heisenberg model. Physical properties are thus controlled by the sublattice magnetization $m(T)$, given *via*

$$m(T) = \frac{1}{2} \tanh\left[\frac{2T_N}{T} m(T)\right], \quad T_N = \frac{1}{4} J_* \tag{2.4}$$

where $T_N = ZJ/4$ ($k_B = 1$) is the Néel temperature. In particular, the probability $\tilde{P}(s)$ of generating an arbitrary spin configuration, $s = \{\sigma_k\}$, is given by an independent product

$$\tilde{P}(s) = \prod_k p_k(\sigma_k), \tag{2.5a}$$

reflecting the statistical independence of the sites for d^∞ (and with finite-d corrections readily shown to be $O(1/d)$). Here $p_k(\sigma_k)$ is the probability that site k is occupied by a σ_k-spin, given in terms of the magnetization by

$$p_k(\sigma_k) = \frac{1}{2}[1 + 2\lambda_k \sigma_k m(T)] \tag{2.5b}$$

where $\lambda_k = +1(-1)$ for sites k belonging to the $A(B)$ sublattice and $\sigma_k = +1(-1)$ for $\uparrow$ ($\downarrow$) spins. In the following we shall often denote $p_k(\sigma) = p_{\alpha\sigma}$ for site k belonging to the $\alpha = A$ or B sublattice, with $p_{A\sigma} = p_{B-\sigma}$ from equation (2.5b). For $T = 0$, where the magnetization $m(T = 0) = \frac{1}{2}$ is saturated, $p_{A\uparrow} = 1 = p_{B\downarrow}$ and $p_{A\downarrow} = 0 = p_{B\uparrow}$, whence as expected equation (2.5a) shows only the Néel spin configuration to be thermally possible. In the paramagnetic phase for $T \geq T_N$ by contrast, $m(T) = 0$ and $p_{\alpha\sigma} = \frac{1}{2}$ $\forall \alpha, \sigma$; all spin configurations are thus equally probable. Equation (2.5) is central to the following analysis of hole dynamics in the $t-J$ model. We shall also require the energy changes, arising from the exchange fields generated by $\hat{H}_J$, upon (i) flipping a spin on site k from σ_k to $-\sigma_k$, and (ii) removing the σ_k-spin. From elementary considerations these are given respectively by $\lambda_k \sigma_k \omega_p(T)$ and $\frac{1}{2}\lambda_k \sigma_k \omega_p(T)$, where

$$\omega_p(T) = J_* m(T). \tag{2.6}$$

2.1 Green functions

To motivate the hole Green functions that we analyze explicitly, we consider first the usual time-ordered single-particle Green function at precisely half-filling (one electron/site). This is given by

$$\tilde{G}_{ii;\sigma}(t) = -i \left\langle \hat{T} \left(\tilde{c}_{i\sigma}(t) \tilde{c}^{\dagger}_{i\sigma} \right) \right\rangle \tag{2.7}$$

with $\hat{T}$ the Wick time-ordering operator; and where $\langle \hat{A} \rangle = \mathrm{Tr}(\hat{A} e^{-\beta \hat{H}})/\mathrm{Tr}\, e^{-\beta \hat{H}}$ with the trace over all states $\{|\Phi_s\rangle\}$ of the half-filled system. Since double occupancy is strictly precluded, it follows that (i) $e^{\lambda \hat{H}}|\Phi_s\rangle = e^{\lambda \hat{H}_J}|\Phi_s\rangle = e^{\lambda \mathcal{E}_s}|\Phi_s\rangle$ for λ an arbitrary c-number, with $\mathcal{E}_s$ the energy of $|\Phi_s\rangle$ under $\hat{H}_J$; (ii) only the advanced ($t \leq 0$) component of $\tilde{G}_{ii;\sigma}(t)$ survives. Hence

$$\tilde{G}_{ii;\sigma}(t) = i\theta(-t) \sum_s \tilde{P}(s) \langle \Phi_s | \tilde{c}^{\dagger}_{i\sigma} e^{i(\hat{H} - \mathcal{E}_s)t} \tilde{c}_{i\sigma} | \Phi_s \rangle \tag{2.8}$$

with $\theta(x)$ the unit step function and $\tilde{P}(s) = e^{-\beta \mathcal{E}_s} / \sum_s e^{-\beta \mathcal{E}_s}$ given by equation (2.5). For $\tilde{c}_{i\sigma}|\Phi_s\rangle$ to be non-vanishing, the spin on site i in $|\Phi_s\rangle$ must be $\sigma_i = \sigma$; *i.e.* $\tilde{c}_{i\sigma}|\Phi_s\rangle = \delta_{\sigma_i \sigma}|i;s\rangle$ where $|i;s\rangle$, with energy E_s under $\hat{H}_J$, denotes a state with a hole on site i and configuration $s = \{\sigma_{k \neq i}\}$ for the remaining spins. From equation (2.5),

$$\tilde{P}(s) = p_i(\sigma_i) P(s) \tag{2.9}$$

where $P(s) = \prod_{k(\neq i)} p_k(\sigma_k) \left(= e^{-\beta E_s} / \sum_{s'} e^{-\beta E_{s'}} \right)$ is the probability of generating $s = \{\sigma_{k \neq i}\}$. Equation (2.8) thus becomes

$$\tilde{G}_{ii;\sigma}(t) = i\theta(-t) p_i(\sigma) \sum_s P(s) \langle i;s | e^{i(\hat{H} - \mathcal{E}_s)t} | i;s \rangle. \tag{2.10}$$

$\mathcal{E}_s$ and E_s differ solely by the energy change (under $\hat{H}_J$) in removing the σ-spin from site i, as considered above; hence $E_s = \mathcal{E}_s + \frac{1}{2}\lambda_i \sigma \omega_p(T)$. Transforming to the frequency domain

$$\tilde{G}_{ii;\sigma}(\omega) = \int_{-\infty}^{\infty} dt e^{i(\omega - i\eta)t} \tilde{G}_{ii;\sigma}(t)$$

where $\eta = 0+$, equation (2.10) thus gives

$$-\tilde{G}_{ii;\sigma}(-\omega) = p_i(\sigma) \overline{G}_{ii} \left(z - \frac{1}{2} \lambda_i \sigma \omega_p(T) \right) \tag{2.11}$$

with $z = \omega + i\eta$; where

$$\overline{G}_{ii}(z) = \sum_s P(s) G_{ii}(z) \tag{2.12a}$$

$$G_{ii}(z) = \langle i;s | [z - \hat{H}']^{-1} | i;s \rangle \tag{2.12b}$$

and

$$\hat{H}' = \hat{H} - E_s. \tag{2.12c}$$

$G_{ii}(z)$ is the hole Green function for an arbitrary spin configuration $s = \{\sigma_{k \neq i}\}$, with $\overline{G}_{ii}(z)$ its thermal average. It is the hole Green function that we consider; from equation (2.11) the time-ordered functions at half-filling follow simply from it (see also Eq. (2.22) below). Note from equations (2.12b,c) that the 'energy origin' for $G_{ii}(z)$ is the energy E_s, under $\hat{H}_J$, of the particular spin configuration $s = \{\sigma_{k \neq i}\}$ being considered. Hence in the atomic limit $t = 0$, where $\hat{H} = \hat{H}_J$, $G_{ii}(z) = 1/z$ for *any* spin configuration; likewise, since $\sum_s P(s) = 1$, $\overline{G}_{ii}(z) = 1/z$.

2.2 Solution for the hole Green function

To analyze the hole Green function, we first decompose the resolvent operator $\hat{G}(z) = (z - \hat{H}')^{-1}$ as

$$\hat{G}(z) = \hat{G}_0(z) + \hat{G}(z) \hat{H}_t \hat{G}_0(z) \tag{2.13}$$

where $\hat{G}_0(z) = (z - \hat{H}'_J)^{-1}$, with $\hat{H}'_J = \hat{H}_J - E_s$, has solely diagonal matrix elements: $\langle k;s'' | \hat{G}_0(z) | i;s \rangle = \delta_{ik} \delta_{ss''}/z$. The non-vanishing matrix elements of $\hat{H}_t$ are $\langle j;s' | \hat{H}_t | i;s \rangle = t_{ji}$, where the spin configurations s' differs from s only by a single electron/hole transfer. Taking matrix elements of equation (2.13) between $\langle i;s|$ and $|i;s\rangle$ then gives

$$z G_{ii}(z) = 1 + \sum_j G_{ij}(z) t_{ji} \tag{2.14a}$$

where

$$G_{ij}(z) = \langle i;s | (z - \hat{H}')^{-1} | j;s' \rangle. \tag{2.14b}$$

The resolvent operator in equation (2.14b) may itself be iterated perturbatively in t using equation (2.13). This amounts to the Nagaoka path formalism, as employed originally for the $J = 0$ limit [3,4]; it yields $G_{ii}(z)$ as an explicit function of frequency, $z = \omega + i\eta$.

We adopt a different strategy, focusing on the Feenberg self-energy $S_i(z)$ defined by

$$G_{ii}(z) = \left[z - S_i(z) \right]^{-1}. \tag{2.15}$$

The Feenberg perturbation series for $S_i(z)$ [20] has been much studied in the context of tight binding models (see *e.g.* [21]). Its unrenormalized form, wherein $S_i(z)$ is expressed as an explicit function of z, is equivalent in the present context to the Nagaoka path formalism; little is therefore gained with it. The general power of the Feenberg perturbation series is however to express $S_i(z)$ in *renormalized* form, *i.e.* as an explicit functional of the $\{G^{(i)}_{jj}, G^{(i,j)}_{kk}, \dots\}$, where for finite-$d$ in general $G^{(i,j\cdots)}_{kk}$ denotes a diagonal Green function with sites $(i,j,\dots)$ removed from the system. In the d^{∞} limit the site removal restrictions are irrelevant, vanishing at least as $O(1/d)$; *e.g.* $G^{(i)}_{jj} = G_{jj} + O(1/d)$ for sites i,j NN's. The Feenberg renormalized perturbation series thus expresses S_i

as a functional of the $\{G_{jj}\}$, hence enabling from equation (2.15) a self-consistent solution for the $\{G_{jj}\}$, as desired and now considered.

Combining equations (2.15) and (2.14a) gives

$$G_{jj}(z)S_i(z) = \sum_j G_{ij}(z)t_{ji} \tag{2.16}$$

in which the explicit dependence upon z in equation (2.14a) has been eliminated. This equation is general, and not confined to the case where t_{ij} connects only NN sites; but for the t–J model itself, knowledge solely of the nearest neighbour off-diagonal Green function G_{ij} (Eq. (2.14b)) as a functional of the $\{G_{jj}\}$ is sufficient to give $S_i \equiv S_i[\{G_{jj}\}]$. This is particularly straightforward for the Bethe lattice (BL) that we consider explicitly here. There are Z terms on the right hand side of equation (2.16) (with Z the coordination number). For the BL, $G_{ij}(z)$ must contain at least one t-bond between the NN sites i and j, and $t = t_*/\sqrt{Z}$. Hence, to recover $S_i(z)$ to $O(1)$ as $Z \to \infty$, we require contributions to $G_{ij}(z)$ with one and only one t-bond. From this it follows, in direct parallel to the corresponding result for a tight binding model (see *e.g.* [21]), that

$$G_{ij}(z) = G_{ii}(z)t_{ij}\langle j;s'|(z-\hat{H}')^{-1}|j;s'\rangle. \tag{2.17a}$$

The state $|j;s'\rangle$, with energy $E_{s'}$ under $\hat{H}_J$, differs from $|i;s\rangle$ only by the *single* hole transfer in which a σ_j-spin electron has been transfered from site j to site i, see Figure 1. Since sites j and i are nearest neighbours, and hence on different sublattices, the spin-energy change due to this electron/hole transfer is thus equivalent to that for flipping a spin on site j from $+\sigma_j$ to $-\sigma_j$, as considered above (see Eq. (2.6)). Hence $E_{s'} = E_s + \lambda_j\sigma_j\omega_p(T)$, reflecting either the energy cost ($\lambda_j\sigma_j = +1$) or gain ($\lambda_j\sigma_j = -1$) due to single-step hole motion, and $(z-\hat{H}')^{-1} = (z - \lambda_j\sigma_j\omega_p(T) - [\hat{H} - E_{s'}])^{-1}$. From this it follows straightforwardly that $\langle j;s'|(z-\hat{H}')^{-1}|j;s'\rangle = G_{jj}(z-\lambda_j\sigma_j\omega_p(T))$, whence equation (2.17a) becomes

$$G_{ij}(z) = G_{ii}(z)t_{ij}G_{jj}(z-\lambda_j\sigma_j\omega_p(T)). \tag{2.17b}$$

Equation (2.16) thus gives $S_i(z)$ as a functional of the $\{G_{jj}\}$, *viz.*

$$S_i(z) = \sum_j t_{ij}^2 G_{jj}(z-\lambda_j\sigma_j\omega_p(T)). \tag{2.18a}$$

For d^∞ the self-energy $S_i(z)$ is of course self-averaging, and for any spin configuration s a fraction $p_j(\sigma)$ of the $Z \to \infty$ sites j that are NN to i have $\sigma_j = \sigma$. Hence, since $t^2 = t_*^2/Z$,

$$S_i(z) = t_*^2 \sum_\sigma p_j(\sigma)\overline{G}_{jj}(z-\lambda_j\sigma\omega_p(T)); \tag{2.18b}$$

from equations (2.15) and (2.12a) the hole Green function is likewise self-averaging, $G_{ii}(z) = \overline{G}_{ii}(z)$. Denoting $\overline{G}_{ii}(z) = G_\alpha(z)$ for site i on the $\alpha = A$ or B sublattice, and likewise $S_i(z) = S_\alpha(z)$, equations (2.18b) and (2.15) thus yield

$$G_\alpha(z) = \left[z - t_*^2 \sum_\sigma p_{\bar{\alpha}\sigma} G_{\bar{\alpha}}(z - \lambda_{\bar{\alpha}}\sigma\omega_p(T))\right]^{-1} \tag{2.19}$$

with $\bar{\alpha} = B(A)$ for $\alpha = A(B)$.

Since $p_{\alpha\sigma} = p_{\bar{\alpha}-\sigma}$ and $\lambda_{\bar{\alpha}} = -\lambda_\alpha$, equation (2.19) shows that $G_\alpha(\omega) = G_{\bar{\alpha}}(\omega) \equiv G(\omega)$: the hole Green function is independent of the sublattice, as is obvious physically. Equation (2.19) thus becomes

$$G(z) = \left[z - t_*^2\left(p_{B\downarrow}G(z-\omega_p(T)) + p_{B\uparrow}G(z+\omega_p(T))\right)\right]^{-1}. \tag{2.20}$$

This is the desired equation for the hole Green function on a Bethe lattice, with $p_{B\sigma}(= p_{A-\sigma})$ and $\omega_p(T)$ given by equations (2.5b, 2.6) in terms of the magnetization $m(T)$, whose dependence on T and J_* in turn follows explicitly from equation (2.4). The limits of equation (2.20) are well-known. For the $T = 0$ string-pinned limit, where $p_{B\sigma} = \delta_{B\downarrow}$ and $\omega_p(0) = \frac{1}{2}J_*$, it reduces to

$$G(z) = \left[z - t_*^2 G(z - \frac{1}{2}J_*)\right]^{-1} \quad : \quad T = 0, \tag{2.21a}$$

originally obtained by Kane, Lee and Read [8] as an approximation in finite-d and later shown by Strack and Vollhardt [15] to be exact for d^∞ at $T = 0$. For $T \geq T_N = \frac{1}{4}J_*$ in the paramagnet, by contrast, $m(T) = 0 = \omega_p(T)$ and $p_{\alpha\sigma} = \frac{1}{2}$, whence equation (2.20) reduces to

$$G(z) = \left[z - \frac{1}{2}t_*^2 G(z)\right]^{-1} \quad : \; T \geq T_N \tag{2.21b}$$

where it is equivalent to the well-known result for $J_* = 0$ [4,14] and produces the semielliptic spectrum of full width $4t_*$ characteristic of free hole motion in the d^∞ BL.

Equation (2.20) is of course exact for all T, bridging the extreme behaviours of the string-pinned limit and free hole motion, the evolution between which naturally occurs on the low-energy scale of $T_N = \frac{1}{4}J_*$ at which AFLRO is melted out. And its physical content is transparent, involving just the probability ($p_{B\sigma}$'s) with which a NN site to the initially created hole is occupied by a σ-spin electron, and the associated energy cost (the $z-\omega_p(T)$ shift) or gain ($z+\omega_p(T)$) under single-step hole transfer. Illustrative results for the T and J_* dependences of the corresponding hole spectra will be given in Section 3.

Finally, note from equation (2.11) that the half-filled time-ordered Green functions $\tilde{G}_{ii;\sigma}(\omega) = \tilde{G}_{\alpha\sigma}(\omega)$ ($\alpha = A$ or B) follow directly from the hole Green function, but in contrast to the hole Green function naturally depend on the sublattice. Since $p_{A\sigma} = p_{B-\sigma}$, equation (2.11) gives

$$\tilde{G}_{A\sigma}(\omega) = \tilde{G}_{B-\sigma}(\omega), \tag{2.22a}$$

with

$$-\tilde{G}_{A\uparrow}(-\omega) = p_{A\uparrow}G(z - \frac{1}{2}\omega_p(T)) \tag{2.22b}$$

$$-\tilde{G}_{A\downarrow}(-\omega) = p_{A\downarrow}G(z + \frac{1}{2}\omega_p(T)). \tag{2.22c}$$

The corresponding majority ($A\uparrow$) and minority ($A\downarrow$) spectra differ trivially by (i) an overall thermal weighting ($p_{A\sigma} = \frac{1}{2}[1 + 2\sigma m(T)]$), and (ii) a net shift of $\frac{1}{2}\omega_p(T) = \frac{1}{2}J_* m(T)$.

2.3 Dynamical conductivity

To calculate the real part of the dynamical hole conductivity, $\sigma(\omega, T)$, we start (as in [15]) from the basic equations of Rice and Zhang [22], obtained from the Kubo formula and valid in any dimension; *viz.*

$$\sigma(\omega,T) = \frac{\left(e^{-\beta\omega}-1\right)}{4\pi\omega VQ} \sum_{q_1,q_2=\pm 1} I(\omega;q_1,q_2) \tag{2.23}$$

with Q the partition function, V the system volume and $I(\omega;q_1,q_2)$ given by

$$I(\omega;q_1,q_2) = \int_{-\infty}^{\infty} d\omega_1 e^{-\beta\omega_1} \,\mathrm{Tr}\left[(\omega_1 + iq_1\eta - \hat{H})^{-1} \times \hat{J}_\delta(\omega_1+\omega+iq_2\eta-\hat{H})^{-1}\hat{J}_\delta\right] \tag{2.24}$$

where

$$\hat{J}_\delta = ieta\sum_{j,\sigma}\left(\tilde{c}^\dagger_{j+\delta,\sigma}\tilde{c}_{j,\sigma} - \tilde{c}^\dagger_{j-\delta,\sigma}\tilde{c}_{j,\sigma}\right) \tag{2.25}$$

is the current operator in an arbitrary direction δ, and Tr is over all single-hole states.

To obtain an exact expression for $\sigma(\omega,T)$ in infinite-d, we consider first the partition function $Q = \mathrm{Tr}e^{-\beta\hat{H}}$ given by

$$Q = \int_\Gamma \frac{dz}{2\pi i} e^{-\beta z}\mathrm{Tr}\left[(z-\hat{H})^{-1}\right] \tag{2.26}$$

with Γ a counterclockwise contour enclosing all singularities of the integrand; and, since all L lattice sites are equivalent, $\mathrm{Tr}[(z-\hat{H})^{-1}] = L\sum_s \langle i;s|(z-\hat{H})^{-1}|i;s\rangle$. Transforming the variable in equation (2.26) to $z' = z - E_s$, with E_s the 'spin only' energy of $|i;s\rangle$ under $\hat{H}_J$, and using equation (2.12a) for the averaged hole Green function $\overline{G}_{ii}(z)$, gives

$$Q = Q_0 L\int_\Gamma \frac{dz}{2\pi i} e^{-\beta z}\overline{G}_{ii}(z) \tag{2.27a}$$

$$= Q_0 L\int_{-\infty}^{\infty} d\omega e^{-\beta\omega} D(\omega) \tag{2.27b}$$

where $Q_0 = \sum_s e^{-\beta E_s}$ is the partition function for the spin background alone. Equation (2.27b) follows, using Cauchy's theorem, from the Hilbert transform

$$\overline{G}_{ii}(z) = \int_{-\infty}^{\infty} d\omega \frac{D(\omega)}{z-\omega} \tag{2.28}$$

where $D(\omega) = -\frac{1}{\pi}\mathrm{Im}\,\overline{G}_{ii}(z=\omega+i\eta)$ is the corresponding hole spectrum.

Proceeding analogously for $I(\omega;q_1,q_2)$, we transform the variable in equation (2.24) to $\omega_1' = \omega_1 - E_s$, obtaining

$$I(\omega;q_1,q_2) = Q_0 L\int_{-\infty}^{\infty} d\omega_1' e^{-\beta\omega_1'} \times K(z_1 = \omega_1' + iq_1\eta; z_2 = \omega_1' + \omega + iq_2\eta) \tag{2.29a}$$

where

$$K(z_1;z_2) = \sum_s P(s)\langle i;s|(z_1-\hat{H}')^{-1}\hat{J}_\delta(z_2-\hat{H}')^{-1}\hat{J}_\delta|i;s\rangle \tag{2.29b}$$

with $\hat{H}' = \hat{H} - E_s$ (Eq. (2.12c)). Equation (2.29b) reduces in turn to

$$K(z_1;z_2) = \sum_s\sum_j P(s)\langle i;s|(z_1-\hat{H}')^{-1}|i;s\rangle\langle i;s|\hat{J}_\delta|j;s'\rangle \times \langle j;s'|(z_2-\hat{H}')^{-1}|j;s'\rangle\langle j;s'|\hat{J}_\delta|i;s\rangle, \tag{2.30}$$

where (as in Sect. 2.2) j is a NN site to i connected to it by the current operator $\hat{J}_\delta$, and the spin configuration s', with energy $E_{s'}$ under $\hat{H}_J$, differs from s solely by the resultant single electron/hole transfer. Equation (2.30) holds for the following reasons. First, the matrix elements of the current operator are given by $\langle i;s|\hat{J}_\delta|j;s'\rangle = \langle j;s'|\hat{J}_\delta|i;s\rangle^* = ieta(\delta_{j,i+\delta} - \delta_{j,i-\delta})$, and are thus proportional to $t = t_*/\sqrt{Z}$. In consequence, as is well-known [15], $\sigma \propto t^2 \sim 1/Z$ is itself proportional to $1/Z$ in large dimensions, but with σ/t^2 (or equivalently $\mathrm{Tr}\sigma_{\delta\delta}(\omega,T)$) of order unity and the quantity we seek in the limit $Z\to\infty$. To recover σ/t^2 to $O(1)$ as $Z\to\infty$ on a Bethe lattice, only diagonal elements of the resolvent operators in equation (2.29b) need be retained. Hence equation (2.30), which can be written equivalently as

$$K(z_1;z_2) = 2(eta)^2\sum_s P(s)G_{ii}(z_1)\langle j;s'|(z_2-\hat{H}')^{-1}|j;s'\rangle \tag{2.31}$$

(and whose form reflects the absence of vertex corrections in d^∞). As discussed in Section 2.2 (Eq. (2.17a)*ff*), $\langle j;s'|(z_2-\hat{H}')^{-1}|j;s'\rangle = G_{jj}(z_2 - \lambda_j\sigma_j\omega_p(T))$; whence, since the spin average in equation (2.31) is uncorrelated in d^∞,

$$K(z_1;z_2) = 2(eta)^2 G(z_1)\sum_\sigma p_{\alpha\sigma}G(z_2 - \lambda_\alpha\sigma\omega_p(T)) \tag{2.32}$$

(where $G(z)\equiv\overline{G}_{ii}(z)$).

Equation (2.32) used in equation (2.29a), together with equations (2.23, 2.27) and the Hilbert transform equation (2.28), lead after a straightforward integration to

the final result for $\tilde{\sigma}(\omega,T) = V\sigma(\omega,T)/2(eta)^2$:

$$\tilde{\sigma}(\omega,T) = \frac{\pi(1-e^{-\beta\omega})}{\omega} \times \frac{\sum_\sigma p_{\alpha\sigma}\int_{-\infty}^{\infty} d\omega_1 e^{-\beta\omega_1} D(\omega_1)D(\omega_1+\omega-\lambda_\alpha\sigma\omega_p(T))}{\int_{-\infty}^{\infty} d\omega_1 e^{-\beta\omega_1}D(\omega_1)} . \tag{2.33}$$

In the $T = 0$ string-pinned limit, where $(p_{B-\sigma} =)p_{A\sigma} = \delta_{A\uparrow}$ and $\omega_p(0) = \frac{1}{2}J_*$, equation (2.33) recovers the result of Strack and Vollhardt [15],

$$\tilde{\sigma}(\omega;0) = \frac{\pi}{\omega}\, D\left(\omega_L + \omega - \frac{1}{2}J_*\right), \tag{2.34}$$

with ω_L the lower band edge of the single-particle spectrum; in particular, as expected physically, the *dc* conductivity vanishes for $T = 0$. For a Bethe lattice, equation (2.33) is however exact in infinite-d for *all* temperatures. And temperature enters it in two ways: (i) explicitly, *via* the trivial thermal factors ($e^{-\beta\omega}$); (ii) implicitly, *via* the T-dependences of $p_{\alpha\sigma}$ (Eq. (2.5b)), $\omega_p(T)$ (Eq. (2.6)) and hence, from equation (2.20), the single-particle spectrum $D(\omega) = -\frac{1}{\pi}\mathrm{Im}G(\omega+i\eta)$. The latter in particular are crucial in a proper description of the T-dependence of the dynamical conductivity (Sect. 4). They are however neglected in the approximate finite-T treatment of Strack and Vollhardt [15], in which only the $T = 0$ Néel spin configuration was used to calculate $\tilde{\sigma}(\omega;T)$, and the limitations of which will shortly become apparent.

2.4 Disorder

Quenched, uncorrelated site-disorder is easily incorporated [15] by addition to the $t-J$ Hamiltonian of

$$\hat{H}_d = \sum_i \epsilon_i\,(\tilde{n}_{i\uparrow} + \tilde{n}_{i\downarrow} - 1)\,, \tag{2.35}$$

where $\tilde{n}_{i\sigma} = \tilde{c}^\dagger_{i\sigma}\tilde{c}_{i\sigma}$ ($\tilde{c}^\dagger_{i\sigma} = c^\dagger_{i\sigma}(1-\hat{n}_{i-\sigma})$) and the $\{\epsilon_i\}$ are independent random variables with a common (normalized) probability density $F(\epsilon_i)$; in practice (Sect. 3) we consider a semi-elliptic disorder distribution of full width $2W$:

$$F(\epsilon) = \frac{2\theta(W-|\epsilon|)}{\pi W}\left[1-(\epsilon/W)^2\right]^{\frac{1}{2}}. \tag{2.36}$$

Inclusion of the c-number term $-\sum_i \epsilon_i$ in equation (2.35) is solely for physical clarity (the disorder potential only being 'felt', when there is a hole on a site); identical results are of course obtained without it.

Since the Heisenberg part of the $t-J$ Hamiltonian is unaffected by the disorder, the analysis of the preceding sections carries over straightforwardly, with thermal averages complemented by a disorder average, $\int\prod_j d\epsilon_j F(\epsilon_j)(\dots)$. The hole Green function is given by (*cf.* Eq. (2.12b)) $G_{ii}(z) = \langle i;s|(z-\hat{H}')^{-1}|i;s\rangle$ where, again, $\hat{H}' = \hat{H} - E_s$ with $\hat{H}$ the full Hamiltonian including $\hat{H}_d$; and such that in the atomic limit ($t = 0$), $G_{ii}(z) = 1/(z+\epsilon_i)$. The Feenberg self-energy is defined by (*cf.* Eq. (2.15)) $G_{ii}(z) = [z+\epsilon_i - S_i(z)]^{-1}$, and trivial extension of the analysis of Section 2.2 shows $S_i(z)$ to be given again by equation (2.18b). In consequence, the full disorder-averaged hole Green function $G(\omega) \equiv \overline{G}_{ii}(z)$ is given exactly by

$$G(z) = \int d\epsilon_i F(\epsilon_i)\left[z+\epsilon_i - t_*^2 \times (p_{B\downarrow}G(z-\omega_p(T)) + p_{B\uparrow}G(z+\omega_p(T)))\right]^{-1} \tag{2.37}$$

and the corresponding time-ordered Green function is again related to $G(\omega)$ by equation (2.22). In the non-disordered limit, $F(\epsilon_i) = \delta(\epsilon_i)$, equation (2.37) reduces to equation (2.20); while in the $T = 0$ limit it reduces to the known result of Strack and Vollhardt [15]. Finally, analysis of the dynamical conductivity is likewise generalized straightforwardly to include disorder: equations (2.33, 2.34) again result for $\tilde{\sigma}(\omega,T)$, with $D(\omega) = -\frac{1}{\pi}\mathrm{Im}G(\omega+i\eta)$ therein given from solution of equation (2.37).

3 Results: single-particle spectra

We consider first the non-disordered case. Equation (2.20) for the Bethe lattice is readily solved by simple iteration, starting form an essentially arbitrary initial form for $G(z)$. In the $T = 0$ string-pinned limit where the sublattice magnetization is saturated ($m(0) = \frac{1}{2}$, see Eq. (2.4)), $G(z)$ is given by solution of equation (2.21a), and the form of the single-particle spectrum $D(\omega) = -\frac{1}{\pi}\mathrm{Im}G(\omega+i\eta)$ is well-known (see *e.g.* [6,8,15]): it consists of a discrete series of lines, reflecting the fact that the hole is strictly localized/confined. Lines at low frequency correspond physically to strings of short length, their separation being of order $t_*[\omega_p(0)/t_*]^{2/3}$ [5,6,15] with $\omega_p(0) = \frac{1}{2}J_*$ (Eq. (2.6)). High frequency lines by contrast correspond to long strings (which naturally have ever decreasing weight on the 'initial' site, and thus diminished spectral intensity); their separation goes asymptotically as $\omega_p(0)$, corresponding simply to the exchange energy penalty incurred upon increasing the string length by one lattice spacing. The $T = 0$ spectrum depends solely on the ratio $\omega_p(0)/t_* = J_*/2t_*$, and with decreasing $\omega_p(0)/t_*$ the spectrum becomes increasingly dense.

For $T \neq 0$ the sublattice magnetization is no longer saturated. From equation (2.4) $m(T)$ — and hence the thermal probabilities $p_{B\sigma} = \frac{1}{2}[1-2\sigma m(T)]$ that enter equation (2.20) for $G(z)$ — is entirely determined by T/T_N with $T_N = \frac{1}{4}J_*$ the Néel temperature. From equation (2.20), noting that $\omega_p(T) = J_* m(T)$, the single-particle spectrum is thus determined by two distinct scales: T/T_N and J_*/t_*. By way of illustration, Figure 2 shows $D(\omega)$ for a fixed $J_*/t_* = 0.5$, at four different temperatures: $T/T_N = 0.3$(a), 0.5(b), 0.7(c) and 0.9(d). For

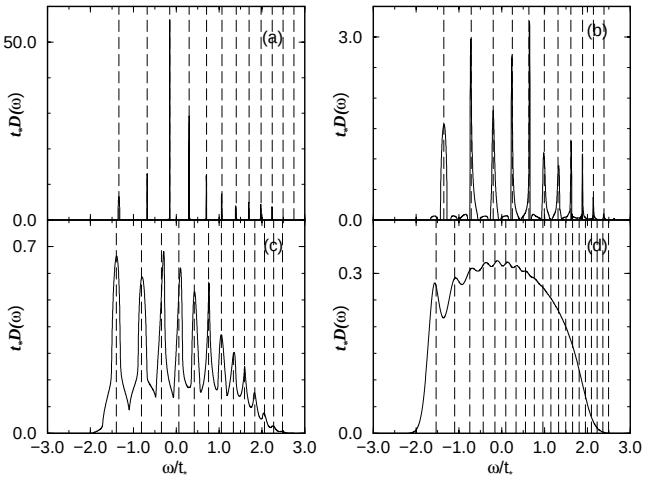

Fig. 2. Single-particle spectra $D(\omega)$ *vs.* ω/t_* for $J_*/t_* = 0.5$ and $T/T_N = 0.3$ (a), 0.5 (b), 0.7 (c) and 0.9 (d). The dashed lines in Figure 2a show the discrete $T = 0$ spectrum; those in Figures 2b to 2d show the fictive $T = 0$ spectra explained in the text.

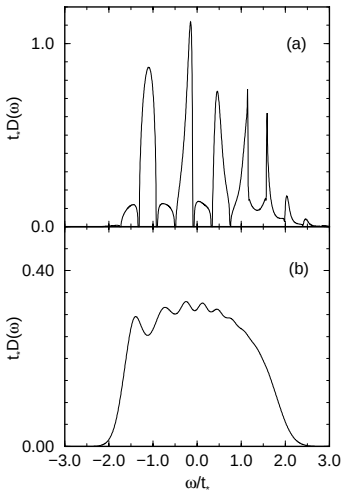

Fig. 3. $D(\omega)$ *vs.* ω/t_* for $J_*/t_* = 1.0$. (a) At $T/T_N = 0.7$ — *cf.* Figure 2c; (b) For the same $\omega_p(T) = J_* m(T)$ as in Figure 2c, here corresponding to $T/T_N = 0.933$.

$T/T_N = 0.3$ the magnetization remains close to saturation, $m(T)/m(0) \simeq 0.9974$, and in Figure 2a we have superimposed the corresponding $T = 0$ spectrum. From this it is clear that $D(\omega)$ resembles closely its $T = 0$ counterpart: the peak positions coincide, and thermal effects merely induce a tiny spectral broadening. This is expected physically since $p_{B\downarrow} \simeq 0.999$, whence from equation (2.20) hole dynamics remain overwhelmingly dominated by majority spin-hops that incur an exchange energy penalty (reflected in the $G(z - \omega_p(T))$ shifts in equation (2.20)).

With increasing T/T_N, however, minority spin-hops that lead to an exchange energy gain become increasingly probable. Their influence upon $D(\omega)$ is already evident by $T/T_N = 0.5$ (Fig. 2b) where $m(T)$ is only modestly reduced to $m(T)/m(0) \simeq 0.96$, corresponding to a minority thermal probability of $p_{B\uparrow} \simeq 0.02$. The spectrum, Figure 2b, is nonetheless significantly different from its $T = 0$ counterpart shown in Figure 2a, with increased thermal broadening and the incipient formation of a background continuum. The latter evolves with increasing T/T_N as illustrated in Figure 2c for $T/T_N = 0.7$ ($m(T)/m(0) \simeq 0.83$ and $p_{B\uparrow} \simeq 0.09$), where $D(\omega)$ has acquired the characteristic of coherent structure superimposed upon an incoherent background, which has important implications for the form and T-dependence of the dynamical conductivity discussed in the following section. With further increasing T/T_N, illustrated in Figure 2d for $T/T_N = 0.9$ ($m(T)/m(0) \simeq 0.53$ and $p_{B\uparrow} \simeq 0.24$), the incoherent background grows at the expense of the coherent peaks, which are gradually destroyed. High frequency coherent structures are the first to be thermally eliminated: as one expects physically since, being due to the longest strings, these are the most susceptible to thermal erosion. Finally, as $T \to T_N-$ where $m(T) \to 0$, all coherent structure is destroyed and $D(\omega)$ acquires the T-independent semielliptic form with full bandwidth $4t_*$ (see Eq. (2.21b)) that is characteristic of the paramagnetic phase for $T > T_N$, reflecting the fact that the hole propagates as a free particle in the paramagnet; the emergence of this behaviour is already apparent in Figure 2d, where the incoherent background is almost semielliptic in form.

To show that, for *all* $T/T_N < 1$, the coherent structure in $D(\omega)$ reflects the exchange energy penalty, $\omega_p(T)$, incurred by majority spin-hops, we superimpose in Figures 2b and 2d the nominal $T = 0$ spectrum that arises by replacing $\omega_p(0) = \frac{1}{2}J_*$ by $\omega_p(T) = J_* m(T)$ with $m(T)$ the magnetization at the actual T/T_N of interest; *i.e.* from solution of equation (2.20) with $p_{B\downarrow} = 1$, $p_{B\uparrow} = 0$ — so that minority spin-hops are suppressed as at $T = 0$ — but with $\omega_p(T)$ given by its value at the T/T_N appropriate to Figures 2b and 2d. Since $m(T)$ diminishes with increasing T/T_N, so does $\omega_p(T)$, whence the density of discrete lines in the fictive $T = 0$ spectra increases with T/T_N. For all T/T_N, it is indeed seen that the positions of the coherent peaks in $D(\omega)$ correspond accurately to those of the nominal $T = 0$ spectra (which would *not* of course be the case if the exact $T = 0$ spectrum — shown in Fig. 2a — was superimposed in Figs. 2b-d).

From the above results is is clear that while the net spectral width is of order $4t_*$ for all T, the character of $D(\omega)$ changes radically on the typically much smaller scale of $T_N = \frac{1}{4}J_*$ over which the controlling spin background evolves from the saturated antiferromagnet to the spin-disordered paramagnet. To exemplify the relative role of J_*/t_* *vs.* T/T_N, Figure 3a shows $D(\omega)$ at $T/T_N = 0.7$ — as in Figure 2c — but for $J_*/t_* = 1$. The sublattice magnetization $m(T)$ (and hence the thermal probabilities $p_{B\sigma}$) thus coincide with that of Figure 2c, but J_* (and hence $\omega_P(T) = J_* m(T)$) has been doubled. The resultant spectrum is seen to be 'cooler' than its counterpart in Figure 2c: naturally, since in doubling $\omega_p(T)$ the exchange energy penalty due to majority spin-hops is amplified. By contrast, again for $J_*/t_* = 1$, Figure 3b shows $D(\omega)$ for the same $\omega_p(T) = J_* m(T)$ as Figure 2c. Since J_* has been doubled, $m(T)$ is halved compared to Figure 2c,

corresponding to a higher temperature ($T/T_N = 0.933$); the resultant spectrum, Figure 3b, is thus 'warmer'.

We note here that Obermeier, Pruschke and Keller [17] have studied the d^∞ $t-J$ model at *finite* hole doping (up to 15%), and within the framework of the Non Crossing Approximation. We suspect, however, that their results at low hole density ($\lesssim 2\%$ or so) may in practice barely differ from the one-hole limit; the NCA determined Néel temperature at 2% doping (Fig. 1 of Ref. [17]), for example, is in fact indistinguishable from $T_N = \frac{1}{4}J_*$ (J^* as used in Ref. [17] is related to J_* used here by $J^* = \frac{1}{2}J_*$). The general features of the NCA spectra, calculated in [17] for the hypercubic lattice, agree qualitatively with those found above; and since the present theory is exact for a single hole, we believe a good assessment of the accuracy of the Non Crossing Approximation could be obtained *via* calculations at as low a hole density as is numerically feasible, and anticipate the NCA to prove rather accurate.

We turn now to the influence of disorder, which at $T = 0$ has been studied by Strack and Vollhardt [15]; and we consider the semielliptic disorder distribution, equation (2.36), with $G(z)$ determined for arbitrary T by solution of equation (2.37). The introduction of disorder at $T = 0$ does not of course change the underlying physics: the hole remains localized, with a vanishing *dc* conductivity (see Eq. (2.34)). Disorder does however lead [15] to inhomogeneous broadening of the erstwhile discrete $t-J$ lines. If the full disorder width $2W < \omega_p(0) = \frac{1}{2}J_*$ — where $\omega_p(0)$ is (for $\omega_p(0)/t_* < 1$) the minimum spacing in the discrete $t-J$ spectrum — then the $t-J$ lines broaden separately and do not overlap. For $2W > \omega_p(0)$, a background continuum will by contrast result. This is illustrated in Figure 4 showing $D(\omega)$ at $T = 0$ for $J_*/t_* = 0.5$ and $W/J_* = 0.5$ (a) and 1 (b), the corresponding discrete spectrum for $W = 0$ being shown in Figure 2a; with increasing disorder the spectrum naturally broadens progressively (tending ultimately to the disorder distribution itself, $D(\omega) = F(\omega)$, in the uninteresting extreme $W \gg 2t_*$).

Comparison of Figure 4a showing disorder-induced inhomogeneous broadening at $T = 0$, with Figure 2b where $W = 0$ and the broadening is purely thermally induced ($T/T_N = 0.5$), shows that disorder — which has some features of additional kinetic energy as noted by Strack and Vollhardt [15] — mimics somewhat the role of temperature. This analogy should not however be pushed far, for two reasons. (i) The underlying physics is quite different in the two cases: for $T = 0$ and any W/t_* the hole remains localized, while at finite-T by contrast the hole is genuinely delocalized with a non-zero static conductivity (discussed in Sect. 4). (ii) $D(\omega)$ is an *averaged* single-particle spectrum, and as such it is not surprising that disparate physical mechanisms — whose effects may be disentangled by analysis of more acute probes of hole dynamics, such as the dynamical conductivity — produce a similar effect upon the averaged Green function. In this regard it is amusing also to note that the effects of a variable *second* NN hopping matrix element on $D(\omega)$ at $T = 0$, as studied by Schiller *et al.* [16], can also mimic the thermal evolution of $D(\omega)$ for the pure $t-J$ model, as seen by comparison of Figures 2c and 2d with Figure 5 of reference [16].

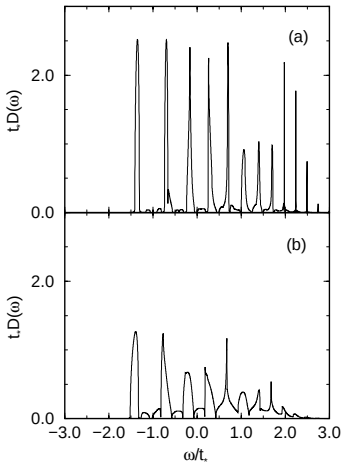

Fig. 4. $D(\omega)$ *vs.* ω/t_* for $T = 0$, $J_*/t_* = 0.5$ and disorder stregths $W/J_* = 0.5$ (a), 1(b). The corresponding spectrum for $W = 0$ is given by the dashed line in Figure 2a.

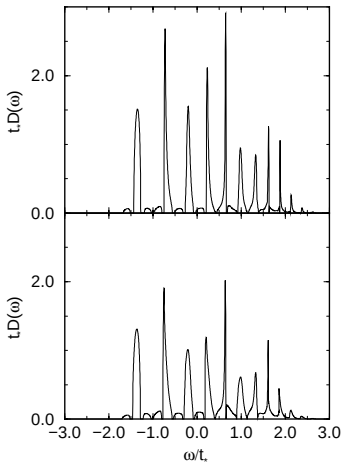

Fig. 5. $D(\omega)$ *vs.* ω/t_* for $T/T_N = 0.5$, $J_*/t_* = 0.5$ with $W/J_* = 0.2$ (a), and 1.0 (b). The corresponding $D(\omega)$ for $W = 0$ is shown in Figure 2b.

Finally we add that the relative influence of disorder upon $D(\omega)$ is strongly T-dependent, and becomes progressively weaker with increasing T/T_N. To illustrate this Figure 5 shows $D(\omega)$ again for $J_*/t_* = 0.5$, with $W/J_* = 0.2$ (a) and 1 (b), but now for $T/T_N = 0.5$ — the $W = 0$ limit of which is shown in Figure 2b. Comparison with Figure 2b shows that, in contrast to the $T = 0$ case (Fig. 4), disorder has only a minor influence on the spectrum over the entire W/t_* range shown, the same being found upon increasing T/T_N.

4 Results: hole conductivity

To illustrate the thermal evolution of the dynamical conductivity, Figure 6 shows the ω-dependence of $\tilde{\sigma}(\omega; T)$

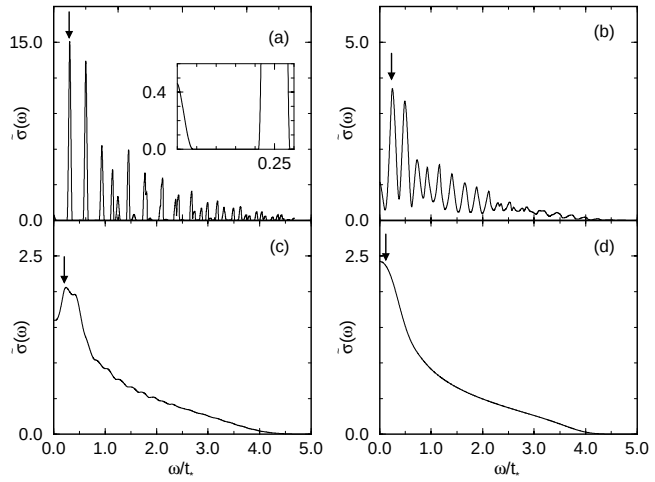

Fig. 6. Dynamical conductivities for $J_*/t_* = 0.5$ and $T/T_N = 0.3$ (a), 0.5 (b), 0.7 (c) and 0.9 (d); $\omega_p(T)$ is marked by a vertical arrow in all cases. The inset to Figure 6a shows the low-frequency behaviour of $\tilde{\sigma}(\omega;T)$ on an expanded scale.

(Eq. (2.33)) for fixed $J_*/t_* = 0.5$ and at four different temperatures: $T/T_N = 0.3$(a), 0.5(b), 0.7(c) and 0.9(d); the corresponding single-particle spectra are given in Figure 2. In the $T = 0$ string-pinned limit the single-particle spectrum $D(\omega)$ is discrete and, since $\tilde{\sigma}(\omega;T=0)$ is given in terms of it by equation (2.34), $\tilde{\sigma}(\omega;0)$ likewise consists of a series of δ-function peaks [15], the first of which occurs at $\omega = \frac{1}{2}J_*(= \omega_p(T=0))$; in particular, as is well-known [15], the the static conductivity naturally vanishes at $T = 0$.

For any $T > 0$ however, the conductivity at low frequencies $\omega \ll \omega_p(T)$ in general, and at $\omega = 0$ in particular, is non-vanishing, reflecting the fact that strict hole confinement/localization is exclusively a $T = 0$ phenomenon. This is directly visible in Figures 6b to 6d (where $\omega_p(T) = J_* m(T)$ is marked by a vertical arrow), and is illustrated most clearly in the expanded inset to Figure 6a for $T/T_N = 0.3$ (where $\omega_p(T)/t_* = 0.2495$ remains exponentially close its $T = 0$ limit of 0.25). Here one sees the emergence of a non-zero $\tilde{\sigma}(\omega;T)$ for frequencies $\omega \ll \omega_p(T)$, separated from the dominant peak centered on $\omega = \omega_p(T)$ (which alone survives at $T = 0$).

The physical origins of this low-frequency behaviour may be understood by first noting that the dominant low-temperature contribution to $\tilde{\sigma}(\omega;T)$ naturally arises from majority spin hops, as reflected in the ω-dependent integral

$$J(\omega) = \int_{-\infty}^{\infty} d\omega_1 e^{-\beta\omega_1} D(\omega_1) D(\omega_1 + \omega - \omega_p(T)) \quad (4.1)$$

contributing to $\tilde{\sigma}(\omega;T)$, equation (2.33). For low temperatures, as discussed in Section 3 and illustrated in Figure 2a for $T/T_N = 0.3$, $D(\omega)$ resembles closely its $T = 0$ counterpart; in particular (see Fig. 2a) the thermally induced spectral broadening is much smaller than the separation between adjacent spectral peaks. In consequence, for frequencies $\omega \ll \omega_p(T) \simeq \omega_p(0) = \frac{1}{2}J_*$, the integrand of equation (4.1) — and hence $\tilde{\sigma}(\omega;T)$ — is in practice non-zero only in an ω_1 range where adjacent spectral lines are separated by an amount of order $\omega_p(T)$. As discussed in Section 3 it is the *high*-frequency lines in $D(\omega_1)$ — associated with long strings — that are thus separated. Hence, as is physically natural, it is these long string states that control the emergent low-frequency conductivity with increasing T from the $T = 0$ string-pinned limit.

The above considerations refer to low frequencies, $\omega \ll \omega_p(T)$. More generally, $J(\omega)$ will be largest for $\omega = \omega_p(T)$ (where there is maximal overlap between the spectral densities in Eq. (4.1)), whence from equation (2.33) one expects $\tilde{\sigma}(\omega;T)$ to be peaked at $\omega = \omega_p(T)$. That this is indeed the case over essentially the entire T/T_N range, is seen from Figure 6 on which $\omega = \omega_p(T)$ is marked (for $T > T_N$, where $\omega_p(T) = 0$, $\tilde{\sigma}(\omega;T)$ decreases monotonically with ω from the static limit).

In qualitative terms, the evolution of $\tilde{\sigma}(\omega;T)$ with temperature (Fig. 6) naturally parallels that of $D(\omega)$ (Fig. 2), although coherent structure in $\tilde{\sigma}(\omega;T)$ is thermally eroded at a lower temperature as seen by comparison of Figures 6c and 6d with Figures 2c and 2d. For temperatures where $\tilde{\sigma}(\omega;T)$ exhibits little coherent structure, the conductivity nonetheless has the rather striking ω-dependence illustrated in Figure 6c for $T/T_N = 0.7$, whereby $\tilde{\sigma}(\omega;T)$ first increases with ω from the static limit, reaches a maximum at $\omega = \omega_p(T)$ and decreases thereafter with increasing ω. This characteristic behaviour persists over an appreciable temperature range, but is naturally destroyed gradually with increasing T/T_N, and $\tilde{\sigma}(\omega;T)$ ultimately becomes a monotonically decreasing function of ω (Fig. 6d). We also note in passing that the exact $\tilde{\sigma}(\omega;T)$, illustrated in Figure 6, is in marked contrast to what arises in an approximation [15] whereby the T-dependences of $p_{\alpha\sigma}, \omega_p(T)$ and $D(\omega)$ are neglected and replaced by their $T = 0$ counterparts (*cf.* Sect. 2.3): here $\tilde{\sigma}(\omega;T)$ at finite-T has exactly the same δ-function ω-dependence as its $T = 0$ limit (but with thermally modified poleweights), and the approximation fails qualitatively to capture the correct ω- or T-dependence of the conductivity.

The examples of Figure 6 refer to a fixed $J_*/t_* = 0.5$, and the dependence upon this ratio again parallels that of $D(\omega)$ described in Section 3; the rule of thumb being that for fixed T/T_N, increasing J_*/t_* produces a somewhat 'colder' $D(\omega)$ or $\sigma(\omega;T)$. This is evident from comparison of Figures 6b and 8a (discussed below), which for fixed $T/T_N = 0.5$ show $\tilde{\sigma}(\omega;T)$ *vs.* ω for $J_*/t_* = 0.5$ and 1 respectively.

The T-dependence of the static conductivity $\tilde{\sigma}_0(T) = \tilde{\sigma}(\omega = 0;T)$, to which we now turn, exemplifies clearly the relative roles of J_* and t_* in the magnetically ordered and paramagnetic phases. Figure 7 shows $\tilde{\sigma}_0(T)$ *vs.* T/t_* for $J_*/t_* = 0.5, 0.8$ and 1.0. For $T > T_N = \frac{1}{4}J_*$ in the paramagnetic phase, $p_{\alpha\sigma} = \frac{1}{2}$ and $\omega_p(T) = 0$ (Eqs. (2.5b, 6)), and $D(\omega)$ is independent of both J_* and T (Eq. (2.21b)). Hence from equation (2.33), $\tilde{\sigma}_0(T)$ in the paramagnet is entirely independent of J_*, depends solely on T/t_* (as seen explicitly in Fig. 7), and reduces to its well-known $J_* = 0$ limit [4,14]: $\tilde{\sigma}_0(T)$ decreases

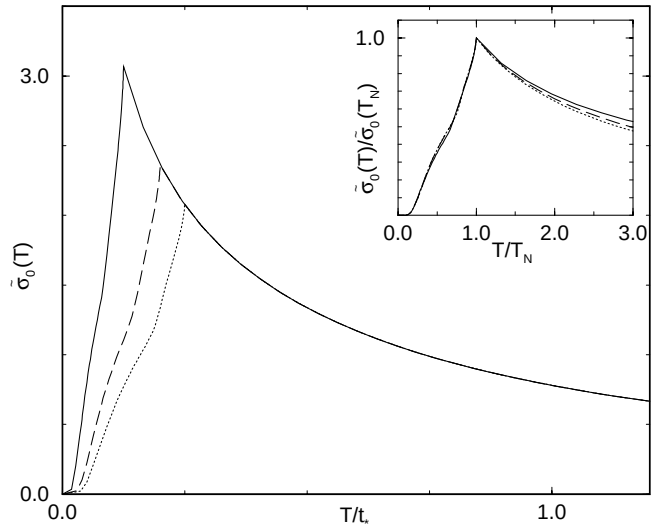

Fig. 7. Static conductivities $\tilde{\sigma}_0(T)$ *vs.* T/t_* for $J_*/t_* = 0.5$ (solid line), 0.8 (dashed) and 1.0 (dotted). Inset: the same results for $\tilde{\sigma}_0(T)/\tilde{\sigma}_0(T_N)$ *vs.* $T/T_N = 4T/J_*$, showing scaling behaviour in the ordered phase.

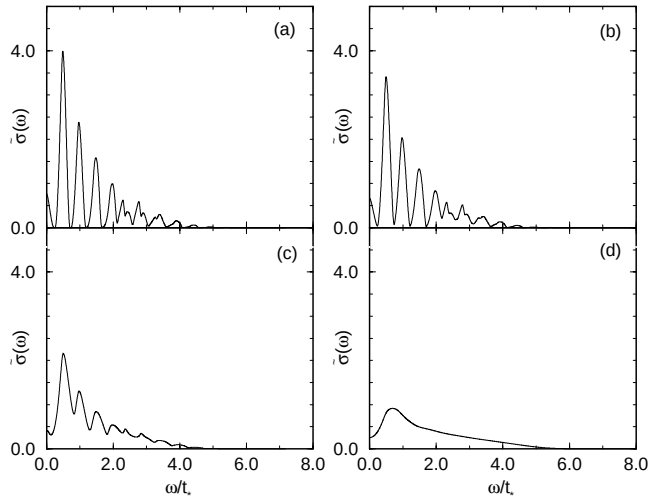

Fig. 8. Dynamical conductivities for $J_*/t_* = 1$ and $T/T_N = 0.5$, with $W/J_* = 0$ (a), 0.2 (b), 0.5 (c) and 1.5 (d).

monotonically with increasing T above T_N, approaching its asymptotic behaviour $\tilde{\sigma}_0(T) \sim 1/T$ on the high temperature 'band' scale $T/t_* \sim 1-2$. In the antiferromagnetic phase, by contrast, it is as expected the much smaller scale $T_N = \frac{1}{4}J_*$, and not the hopping t_*, that sets the scale for the thermal evolution of $\tilde{\sigma}_0(T)$. For $T/T_N \ll 1$, $\tilde{\sigma}_0(T)$ is exponentially small, behaving asymptotically for $T \to 0$ as $\tilde{\sigma}_0(T) \sim \frac{1}{T}\exp(-|\omega_L|/T)$ with $\omega_L = -|\omega_L|$ the lower band edge in $D(\omega)$ (as may be shown from Eq. (2.33)). $\tilde{\sigma}_0(T)$ increases progressively with T throughout the ordered phase, reflecting the enhanced thermal broadening of $D(\omega)$ (Fig.2) and the progressively increasing importance of minority spin hops; and at $T = T_N$ the dc conductivity acquires a sharp cusp across which $d\tilde{\sigma}_0(T)/dT$

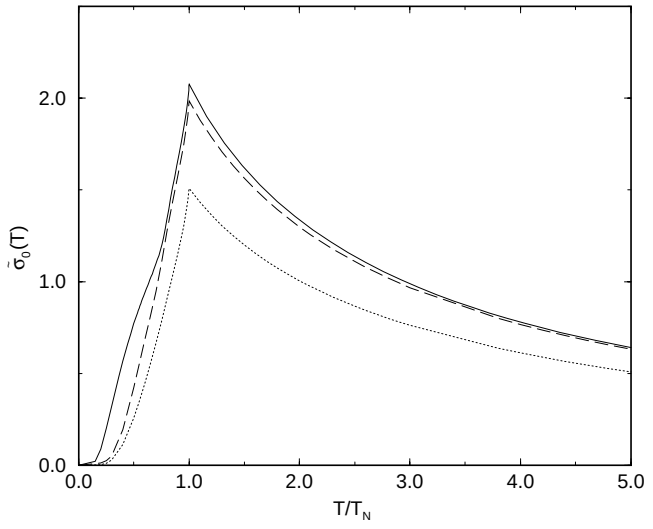

Fig. 9. Static conductivities $\tilde{\sigma}_0(T)$ *vs.* T/T_N for $J_*/t_* = 1.0$ and $W = 0$ (solid line), 0.5 (dashed), 1.5 (dotted).

changes sign to a negative value characteristic of 'clean' hole propagation.

While $\tilde{\sigma}_0(T)$ depends upon both J_* and t_* in the ordered phase $T < T_N$, the dominance of the former scale is evident from the inset to Figure 7, where $\tilde{\sigma}_0(T)/\tilde{\sigma}_0(T_N)$ is now shown as a function of $T/T_N = 4T/J_*$. From this it is seen that for $T/T_N < 1$, $\tilde{\sigma}_0(T)/\tilde{\sigma}_0(T_N)$ is an almost universal function of T/T_N; which 'scaling', while pristine only for $T \simeq T_N$, shows the controlling influence of T/J_* in the antiferromagnet.

Finally, we consider briefly the influence of disorder upon the dynamical conductivity, $\tilde{\sigma}(\omega;T)$ being given again by equation (2.33). Figure 8 shows $\tilde{\sigma}(\omega;T)$ *vs.* ω/t_* for a fixed temperature $T/T_N = 0.5$ with $J_*/t_* = 1$, and for four different disorder strengths W/J_*. Increasing disorder leads as expected to inhomogeneous broadening of the dynamical conductivity and consequent erosion of coherent structure, the effect being somewhat more pronounced than that upon $D(\omega)$ illustrated in Figure 5 (for $J_*/t_* = 0.5$).

Of particular interest is the influence of disorder on the static conductivity $\tilde{\sigma}_0(T)$. For $T = 0$ the dc conductivity is identically zero for all disorder strengths [15] as seen explicitly from equation (2.34), so the question is pertinent only at finite temperature. From Figure 8 it is seen that $\tilde{\sigma}_0(T) = \tilde{\sigma}(\omega = 0;T)$ decreases progressively with increasing disorder strength. This is at variance with the results of Strack and Vollhardt [15], who found a new effect whereby $\tilde{\sigma}_0(T)$ is actually enhanced with increasing disorder over a wide disorder interval; see Figure 13 of reference [15]. Such behaviour arises upon neglect of the T-dependence of $D(\omega)$ in equation (2.33) for $\tilde{\sigma}(\omega;T)$ (as well as that of $p_{\alpha\sigma}$ and $\omega_p(T)$), $D(\omega)$ therein being replaced by its $T = 0$ limit corresponding to retention solely of the Néel spin configuration. This amounts in effect to a rigid band approximation to $D(\omega)$, and since disorder induces a T-independent spectral broadening of the discrete $t-J$ lines arising for $W = 0$, the effect found by Strack

and Vollhardt [15] is readily understood. Unfortunately, it is however an artifact of the underlying approximation: for any finite temperature we find by contrast that the exact static conductivity obtained from equation (2.33) decreases monotonically with increasing disorder, as illustrated in Figure 9 showing $\tilde{\sigma}_0(T)$ *vs.* T/T_N for $J_*/t_* = 1$ and $W/J_* = 0, 0.5$ and 1.5, and in accordance with one's physical expectation that disorder should diminish static hole transport in both the antiferromagnetic and paramagnetic phases.

5 Summary

We have investigated in this paper the thermal evolution of the dynamics of a hole in an antiferromagnetic spin background, as described by the $t-J$ model, and in the limit of large spatial dimensions, $d = \infty$, where an exact solution has been obtained. Resultant single-particle spectra and dynamical hole conductivities exhibit a rich frequency and temperature dependence that reflects the strong variation with temperature, on scales of order $T_N = J_*/4$, of the coupling bewteen hole motion and the spin background; and which exemplify clearly the thermal evolution of the underlying string picture from the $T = 0$ string-pinned limit through to the paramagnetic phase. The additional effects of quenched site disorder have also been included, leading to exact results in infinite-d for the interplay between static disorder and thermally induced hole dynamics.

The underlying methodology — in particular that of the Feenberg renormalized perturbation series (RPS) — is physically transparent, and not confined to the pure $t-J$ model studied here. Equation (2.16) for example is quite general and may be used, in conjunction with the RPS, to investigate *e.g.* the important effects of a second nearest neighbour hole hopping [16]; which even for a Bethe lattice involves non-retraceable loop paths, and likewise admits in $d = \infty$ to an exact solution for all T [23].

Finally, we add that the approach described here in the $d = \infty$ limit may be used as a basis for the development of approximation schemes in finite-d. Work on this problem is currently in progress, but a brief qualitative comment is in order. In $d = \infty$, where simple molecular field theory for the spin background is exact, spin correlations reflect solely (and trivially) long-ranged order, and are entirely absent in the paramagnetic phase. In finite-d, by contrast, significant local antiferromagnetic spin correlations persist well into the paramagnetic phase, being wiped out only on scales $T \gg J$. Thus, even for $T > T_N$, a σ-spin hole is more probably surrounded by $-\sigma$-spins, and an exchange energy penalty or gain may again arise under single-step hole transfer, according to which spin hops. In consequence, even in the paramagnet, one expects the behaviour of *e.g.* $\sigma(\omega; T)$ to exhibit an ω- and T-dependence akin to that found in $d = \infty$ for the ordered phase (see *e.g.* Figs. 6c, 6d), behaviour symptomatic of the persistent strong interaction between the moving hole and the spin background, and to which we will return in a later paper.

MPHS gratefully acknowledges financial support from the FdChI through a Kekulé scholarship.

References

1. F.C. Zhang, T.M. Rice, Phys. Rev. B **37**, 3759 (1988).
2. E. Dagotto, Rev. Mod. Phys. **66**, 763 (1994).
3. Y. Nagaoka, Phys. Rev. **147**, 392 (1966).
4. W.F. Brinkman, T.M. Rice, Phys. Rev. B **2**, 1324 (1970).
5. L.N. Bulaevskii, É.L. Nagaev, D.I. Khomskiĭ, Zh. Eksp. Teor. Fiz. **54**, 1562 (1986) [Sov. Phys. J.E.T.P **27**, 836 (1968)].
6. B.I. Shraiman, E.D. Siggia, Phys. Rev. Lett. **60**, 740 (1988); Phys. Rev. B **42**, 2485 (1990).
7. S. Schmitt-Rink, C.M. Varma, A.E. Ruckenstein, Phys. Rev. Lett. **60**, 2793 (1988).
8. C.L. Kane, P.A. Lee, N. Read, Phys. Rev. B **39**, 6880 (1989).
9. R. Eder, K.W. Becker, Z. Phys. B **78**, 219 (1990).
10. M.M. Mohan, J. Phys.-Cond. **3**, 4307 (1991).
11. S. Trugman, Phys. Rev. B **37**, 1597 (1988).
12. E. Dagotto, R. Joynt, A. Moreo, S. Bacci, E. Cagliano, Phys. Rev. B **41**, 9049 (1990).
13. Z. Liu, E. Manousakis, Phys. Rev. B **45**, 2425 (1992).
14. W. Metzner, P. Schmit, D. Vollhardt, Phys. Rev. B **45**, 2237 (1990).
15. R. Strack, D. Vollhardt, Phys. Rev. B **46**, 13852 (1992).
16. A. Schiller, P. Kumar, R. Strack, D. Vollhardt, Phys. Rev. B **51**, 8337 (1995).
17. T. Obermeier, T. Pruschke, J. Keller, Ann. Physik **5**, 137 (1996).
18. T. Pruschke, Q. Qin, T. Obermeier, J. Keller, J. Phys.-Cond. **8**, 3161 (1996).
19. D.E. Logan, M.P.H. Stumpf, Europhys. Lett. **43**, 207 (1998).
20. E. Feenberg, Phys. Rev. **74**, 206 (1948).
21. E.N. Economou, *Green's Functions in Quantum Physics*, 2nd ed. (Springer, Berlin, 1983).
22. T.M. Rice, F.C. Zhang, Phys. Rev. B **39**, 815 (1989).
23. N.L. Dickens, D.E. Logan, in preparation.